J. Phys. D: Appl. Phys. **33** (2000) 2653–2656. Printed in the UK PII: S0022-3727(00)14675-3

Modelling for size-dependent and dimension-dependent melting of nanocrystals

Z Zhang, J C Li and Q Jiang

Department of Materials Science and Engineering, Jilin University of Technology, Changchun 130025, People's Republic of China

E-mail: jiangq@post.jut.edu.cn

Received 14 June 2000, in final form 11 July 2000

Abstract. A unified model, free of any adjustable parameters, for the size-dependence and dimension-dependence of melting point depression and superheating of nanocrystals is developed. In terms of the consideration of the surface/volume ratio of nanocrystals, the suppression of melting point of nanocrystals and superheating of embedded nanocrystals are predicted. The model predictions for the melting temperatures of nanocrystals are consistent with the experimental results and molecular dynamics simulations.

1. Introduction

The melting of nanocrystals has received considerable attention since Takagi in 1954 experimentally demonstrated that ultrafine metallic nanocrystals melt below their corresponding bulk melting temperature [1]. It is now known that the melting temperature of all low-dimensional crystals, including metallic [2–4], organic [5, 6] and semiconductor [7] depends on their sizes. For free standing nanocrystals, the melting temperature decreases as its size decreases [1–7]. For nanocrystals embedded in a matrix, they can melt below or above the melting point of the corresponding bulk crystal depending on the interface structure between embedded nanocrystals and the matrix [8–14]. If the interfaces are coherent or semi-coherent, an enhancement of the melting point is present. Otherwise, there is a depression of the melting point [13, 14]. Some molecular dynamics (MD) simulations have shown that free clusters exhibit a depression of the melting point as the size decreases [15, 16] while embedded or coated clusters can exhibit superheating [17, 18], depending on the nature of the interfaces. A thorough understanding of the thermal properties of such low-dimensional materials is of importance because of their potential applications in the field of microelectronics, solar energy utilization and nonlinear optics.

Recently, a model for size-dependent melting temperature is developed based on the size-dependent amplitude of the atomic thermal vibrations of nanocrystals in terms of the Lindemann criterion [3–5]. The model has predicted the size-dependent melting for metallic thin films [3], for metallic nanowires [4] and for organic nanocrystals [5]. Since all the parameters in our model are only the well known bulk melting temperature and the bulk melting entropy, our model can predict the size-dependent and dimension-dependent melting temperature of any kind of nanocrystals. The available experimental evidence confirms the predicted results.

In this contribution, the theoretical prediction in terms of the above model is carried out for the size-dependent and dimension-dependent melting of nanocrystals and for the size-dependent superheating of embedded nanocrystals. The correspondence between the theoretical predictions and the experimental results of the melting temperatures of the nanocrystals was found.

2. Model

The $T_m(r)$ function of metallic and organic nanocrystals is described by the following expression [4–7]

$$T_m(r)/T_m(\infty) = \exp[-(\alpha - 1)/(r/r_0 - 1)] \qquad (1)$$

where $T_m(r)$ and $T_m(\infty)$ are the melting temperature of the nanocrystals with radius r and corresponding bulk crystals, respectively. r_0 denotes a critical radius at which all atoms of the particle are located on its surface. α is defined as the ratio of the mean square displacement (msd) of atoms on the surface and that in the interior of crystals [5]. For low-dimensional crystals, r_0 is dependent on the dimension of the crystal d: $d = 0$ for nanocrystals, $d = 1$ for nanowires and $d = 2$ for thin films. In general, the dimension can be fractional [3]. For a nanoparticle, r has the usual meaning of radius. For a nanowire, r is taken as its radius. For a thin film, r denotes its half thickness. r_0 is given by: (1) $r_0 = 3h$ for $d = 0$ since $4\pi r_0^2 h = 4\pi r_0^3/3$; (2) $r_0 = 2h$ for $d = 1$ since $2\pi r_0 h = \pi r_0^2$; and (3) $r_0 = h$ for $d = 2$ since $2h = 2r_0$. In short, the relationship between d and r_0 is [3–5]

$$r_0 = (3 - d)h. \qquad (2)$$

0022-3727/00/202653+04$30.00

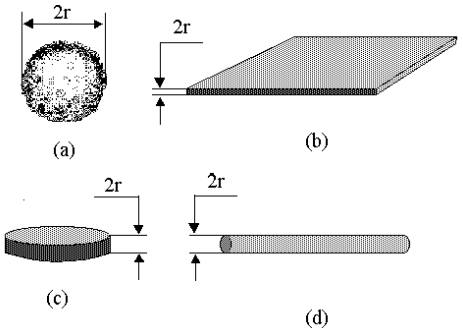

Figure 1. Schematic diagram of four types of low-dimensional nanocrystals. (a) Spherical particles, $d = 0$; (b) thin films, $d = 2$; (c) disc-like particles, $d = 1$ and (d) nanowire, $d = 1$.

Note that if the crystalline structure or co-ordination number of a crystal is different, h varies somewhat. To eliminate this effect, h is calculated by the volume per atom Ω such that $\Omega = \pi h^3/6$ [19]. This method has an additional advantage that the atomic volume is measurable in any structure, no matter how complex, by dividing the volume of the unit cell by the number of atoms in the unit cell.

When a nanoparticle is deposited on an inert substrate, it may wet or not wet the substrate. When the deposit does not wet the substrate, the deposit will prefer taking a spherical shape which has the smallest surface/volume ratio where $d = 0$. When the deposit wets the substrate, an island-like or disc-like particle may arise. The surface/volume ratio of this shape is smaller than the spherical particle since one surface of the disk disappears. In fact, the effective surface area of a disk on the substrate is half of that of a film. For a film, $r_0 = h$. It is not difficult to understand that $r_0 = 2h$ for a disk-like particle, which implies a quasi-dimension of the disk of one with respect to equation (2). To clarify four different shapes of low-dimensional materials, a schematic diagram of above four low-dimensional crystals are shown in figure 1. Although (2) does not consider the wetting details which differ for different deposits and substrates, equation (1) in terms of (2) can predict the $T_m(r)$ function of the nanocrystals when the shape of the nanocrystals are known.

Since a crystal is characterized by its long-range order, the smallest nanocrystal should have at least a half of the atoms located within the nanocrystal. Hence, the smallest r is $2r_0$ [3–5]. One would argue that even for a thin film of a monolayer, it may exist in the crystalline state due to its two-dimensional long-range order. However, all atoms of this thin film are located on the surface and their thermal vibration differs from the bulk crystals. In fact, Mitch *et al* [20] have found that when r of the Bi thin film decreases to 0.4 nm, its crystallinity disappears. This observation is expected based on (2): for Bi, $h = r_0 = 0.20$ nm [21] since $d = 2$, its crystallinity disappears when $r = 2r_0 = 0.40$ nm. For Pb nanowire in carbon nanotubes, $d = 1$, $h = 0.39$ nm [19] and $r_0 = 0.78$ nm, $2r_0 = 1.56$ nm, which again is fully consistent with the observation that the crystallinity of Pb disappears at $r = 1.5$ nm [21].

It is evident from (1) that the $T_m(r)$ function depends on α. If $\alpha > 1$, $T_m(r)/T_m(\infty) < 1$, $T_m(r)$ decreases as r decreases. When $\alpha < 1$, does $T_m(r)/T_m(\infty) > 1$ imply that $T_m(r)$ increases as r increases. For crystals with free surfaces, such as free-standing particles, particles or thin films deposited on inert substrates, and nanowires in porous glasses, their msd of the surface atoms is larger than that of the interior atoms of the nanocrystals and $\alpha > 1$. α can be deduced by the vibrational entropy expression of Mott [25, 26] and expressed as [7]

$$\alpha = [2S_m(\infty)/(3R)] + 1. \tag{3}$$

Substituting (3) into (1), there is

$$T_m(r)/T_m(\infty) = \exp\{-2S_m(\infty)/[3R(r/r_0 - 1)]\}. \tag{4}$$

When nanocrystals are embedded in the matrix, their surface atoms are no longer free-standing. α could be smaller than one due to the interaction on the interfaces between the embedded nanocrystal and the matrix. When the interface is coherent, the msd of the surface atoms of nanocrystals falls between that of the interior atoms of nanocrystals and that of the bulk matrix. It is simple to assume that the msd of atoms on the interface is an averaged msd value of interior atoms of nanocrystals and that of the bulk matrix, α is read as [24]

$$\alpha = \{[h_M^2/h_m^2]T_m(\infty)/T_M(\infty) + 1\}/2 \tag{5}$$

where h_M and h_m are atomic diameters of the matrix and the nanocrystals, respectively. $T_M(\infty)$ denotes the melting temperature of the matrix. In terms of (1) and (5), the size dependence of superheating of the melting temperature of nanocrystals can be predicted.

3. Results and discussions

3.1. Depression of melting temperature of nanocrystals

Figure 2 presents a comparison between the model predictions of (5) and the experimental results of $T_m(r)$ for disc-like particles of Au ($d = 1$) [25] and the MD results of Au nanoparticles ($d = 0$) [16]. As shown in the figure, the theoretical model is in good agreement with both experimental and MD evidence. $T_m(r)$ decreases as r and d decrease.

Figures 3 to 6 give the comparison between our model prediction of (5) and experimental data for spherical ($d = 0$) and disc-like ($d = 1$) particles of Pb [26, 27] (figure 3), Al ($d = 0$) [28] (figure 4), In ($d = 1$ and $d = 0$) [27, 29] (figure 5) and Sn ($d = 1$) [25, 28] and the corresponding thin film ($d = 2$) [30] (figure 6), respectively. It is observed that the melting temperature depression can be induced by both the size and the dimension. Although the sources of the experimental results and the MD simulations are different, it is easy to understand different results from different authors according to our universal model under the consideration of dimension.

Since we have compared the size dependence of the melting temperature for organic nanoparticles elsewhere [5], here we only show a comparison of the size-dependent melting of an inert gas crystal of Ar between our model prediction of (5) and the MD results [15]. We again observed a rather good agreement between our model and the MD results as shown in figure 7.

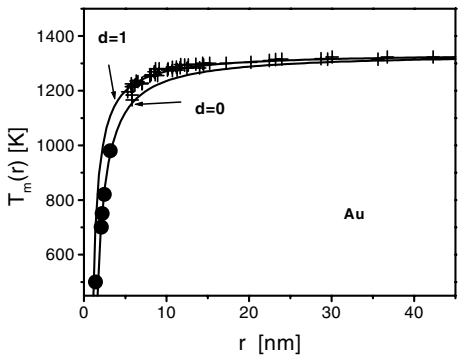

Figure 2. The $T_m(r)$ function of Au nanocrystals in terms of equation (4). For the disk-like nanocrystals, $d = 1$, $r_0 = 2h = 0.6376$ nm with $h = 0.3188$ nm [19], $T_m(\infty) = 1337.58$ K and $S_m(\infty) = 9.38$ J mol^{-1} K^{-1} [34]. For spherical nanoparticles, $d = 0$ and $r_0 = 3h = 0.9564$ nm. + and ● denote the experimental [25] and MD [16] results, respectively.

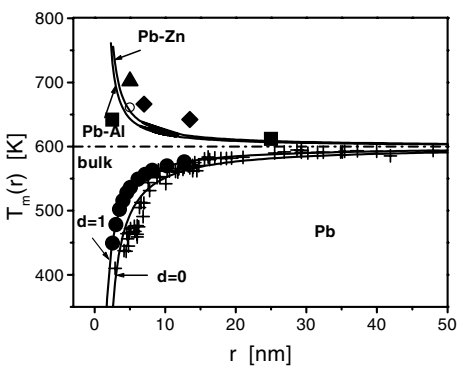

Figure 3. The $T_m(r)$ function of Pb nanocrystals. For disc-like particles, $d = 1$, $r_0 = 2h = 0.7796$ nm with $h = 0.3898$ nm [19], for spherical particles, $d = 0$, $r_0 = 3h = 1.1694$ nm, where $T_m(\infty) = 600.6$ K and $S_m(\infty) = 7.99$ J mol^{-1} K^{-1} [34]. The symbols + and ● denote the measured $T_m(r)$ values [26, 27]. For Pb nanocrystals embedded in an Al matrix, the $T_m(r)$ function is plotted by (1), $\alpha = 0.71$ in terms of (5) where $h_M = 0.3164$ nm [19], $T_M(\infty) = 933.25$ K [34]. The experimental results are plotted as ▲, ■ and ♦ [13, 18, 33]. For Pb nanocrystals embedded in a Zn matrix the $T_m(r)$ function is calculated by (1) with $\alpha = 0.77$ in terms of (5), where $h_M = 0.3076$ nm [19], $T_M(\infty) = 692.73$ K [34]. The symbol ○ denotes the experimental data [15].

These correspondences between our model and the experimental and MD evidence imply that our model bears universally on the melting of different kinds of nanocrystals. The nature of dimension dependence of the melting temperature is the difference of the ratio of the surface atom number and atom number within the nanocrystals. This ratio increases as d decreases.

3.2. Superheating of nanocrystals

The theoretical prediction of (1) and (5) for the superheating of Pb particles is compared with the experimental results in figure 3 where Pb particles are embedded in Al [8, 13, 31] and in the Zn matrix [10]. It is clear that the size dependence of superheating is stronger than the matrix dependence of the superheating. This is possibly due to the small difference of the melting temperatures of Zn and Al. Figure 5 gives $T_m(r)$ function of In nanocrystals embedded in an Al matrix compared with the corresponding experimental results [9, 14, 32, 33]. It is obvious that such predictions in different

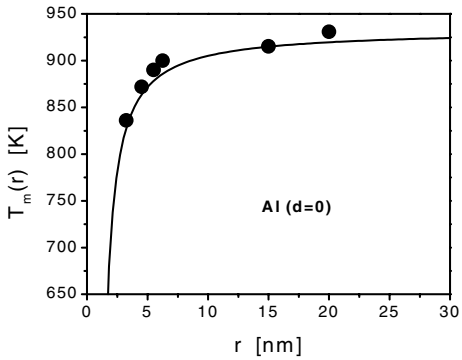

Figure 4. The $T_m(r)$ function of spherical Al nanocrystals in terms of equation (5) where $r_0 = 3h = 0.9492$ nm in terms of (2) with $d = 0$ and $h = 0.3164$ nm [19], $T_m(\infty) = 933.25$ K and $S_m(\infty) = 11.56$ J mol^{-1} K^{-1} [34]. ● denotes the experimental values [28].

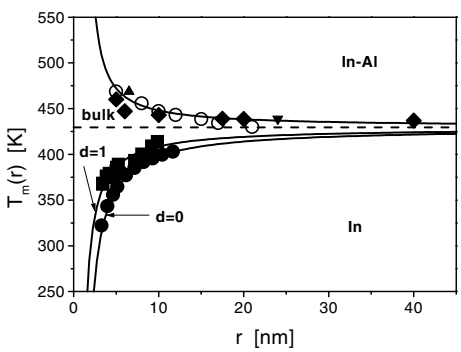

Figure 5. The $T_m(r)$ function of In nanocrystals. For disc-like particles, $d = 1$, $r_0 = 2h = 0.7364$ nm; for spherical particles, $d = 0$, $r_0 = 3h = 1.1046$ nm, where $h = 0.3682$ nm [19], $T_m(\infty) = 429.76$ K and $S_m(\infty) = 7.59$ J mol^{-1} K^{-1} [34]. The symbols ● and ■ denote the measured $T_m(r)$ values [27, 29]. For In nanocrystals embedded in an Al matrix, $T_m(r)$ is obtained by (1), $\alpha = 0.67$ in terms of (5) where $h_M = 0.3164$ nm [19], $T_M(\infty) = 933.25$ K [34]. The experimental evidence is shown as ▼, ▲, ○ and ♦ [9, 14, 32, 33].

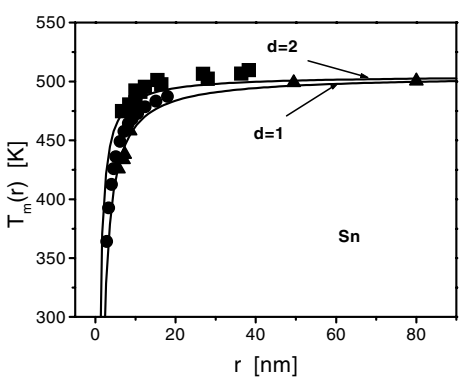

Figure 6. The $T_m(r)$ function of Sn nanocrystals in terms of (4) where $T_m(\infty) = 429.76$ K and $S_m(\infty) = 13.92$ J mol^{-1} K^{-1} [34]. The symbols ●, ▲ and ■ denote the measured $T_m(r)$ values [25, 27, 30]. For the disk-like nanocrystals, $r_0 = 2h = 0.7448$ nm with $h = 0.3724$ nm [19], for thin films, $d = 2$, and $r_0 = h = 0.3724$ nm in terms of (2).

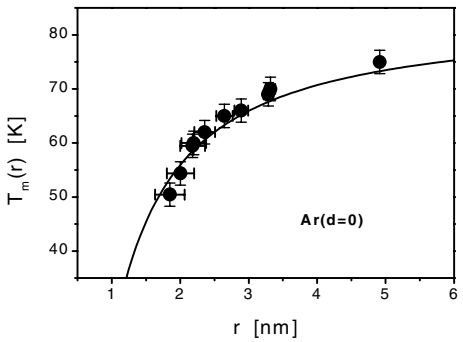

Figure 7. Comparison between the model prediction of (4) (full curve) and MD results (●) [15] for Ar nanoparticles where $r_0 = 3h = 0.528$ nm in terms of (2) since $d = 0$ and $h = 0.176$ nm [34], $T_m(\infty) = 83.81$ K and $S_m(\infty) = 14.18$ J g atom^{-1} K^{-1} [34].

systems give a good agreement with the experimental data of different authors.

As shown in figures 3 and 5, only when $\alpha < 1$, $T_m(r)/T_m(\infty) > 1$ does $T_m(r)$ increase as r decreases. $\alpha < 1$ implies that the effect of compressive force is essentially on the surface atoms of the nanocrystals. Thus, the stress induced by the matrix on the nanocrystals is inhomogeneous. As r decreases, the percentage of the surface atoms of the nanocrystals increases, and thus, the effect of the stress increases too.

Because there is agreement between the model prediction and experimental results, equation (5) should be reasonable. In terms of (5), when $\alpha < 1$, $T_m(\infty)/T_M(\infty) < h_m^2/h_M^2$. While $T_m(\infty)/T_M(\infty) < 1$ is necessary and understandable for the superheating, $h_m/h_M > 1$ in all reported systems (see the figure captions in figures 3 and 5). It is plausible if $h_m/h_M < 1$, the local internal stress on the interface is a tensile one, which increases but does not decrease the msd of the surface atoms of the nanocrystals. Thus, any evident superheating should occur only when $h_M^2/h_m^2 < 1$ although this is not a necessary condition for $\alpha < 1$ in (5).

4. Summary

In conclusion, a simple model based on the enhancement or the suppression of thermal vibrations of atoms on the surface (or the interface) of nanocrystals is developed to account for size-dependent and dimension-dependent melting. For free-standing nanocrystals, the melting behaviour depends on the size, the dimension and α. Although (5) as a function of crystal size is derived by formally extending Mott's estimate of the melting entropy of an infinite metallic crystal to metallic crystals of finite size, they can be utilized for nanocrystals whose melting behaviour are dominated by vibration. Reasonable agreement has been found between the experimental data of free-standing metallic nanocrystals and the model prediction.

For nanocrystals embedded in a matrix, the necessary conditions for the superheating of the nanocrystals are that $\alpha < 1$, the matrix has a higher melting temperature than the embedded crystals in the bulk have and there are the coherent or semi-coherent interfaces between them, which decreases the msd of the surface atoms of the embedded nanocrystals. Another sufficient, but not necessary condition is that the atomic diameter of the matrix is smaller than that of the nanocrystals. Experimental evidence confirms the present model.

Acknowledgments

The financial support of the National Natural Science Foundation of China under grant No 59931030 and the Trans-Century Training Program Foundation for the Talents by the Ministry of Education of China are acknowledged.

References

[1] Takagi M 1954 *J. Phys. Soc. Japan* **9** 359
[2] Hasegawa M, Hoshino K and Watabe M 1980 *J. Phys. F: Met. Phys.* **10** 619
[3] Jiang Q, Tong H Y, Hsu D T, Okuyama K and Shi F G 1998 *Thin Solid Films* **312** 357
[4] Jiang Q, Aya N and Shi F G 1997 *Appl. Phys.* A **64** 627
[5] Jiang Q, Shi H X and Zhao M 1999 *J. Chem. Phys.* **111** 2176
[6] Morishige K and Kawano K 1999 *J. Phys. Chem.* B **103** 7906
[7] Goldstein A N 1996 *Appl. Phys.* A **62** 33
[8] Chattopadhyay K and Goswami R 1997 *Prog. Mater. Sci.* **42** 287
[9] Zhang D L and Cantor B 1991 *Acta Metall. Mater.* **39** 1595
[10] Goswami R and Chattopadhyay K 1993 *Phil. Mag. Lett.* **68** 215
[11] Thoft N B, Bohr J, Buras B, Johnson E and Johansen A 1995 *J. Phys. D: Appl. Phys.* **28** 539
[12] Dybkjaer G, Kruse N, Johansen A, Johnson E, Sarholt-Kristensen L and Bourdelle K K 1996 *Surf. Coat. Tech.* **83** 82
[13] Sheng H W, Ren G, Peng L M, Hu Z Q and Lu K 1996 *Phil. Mag. Lett.* **73** 179
[14] Sheng H W, Ren G, Peng L M, Hu Z Q and Lu K 1997 *J. Mater. Res.* **12** 119
[15] Ercikessum F, Andreoni W and Tosatti E 1991 *Phys. Rev. Lett.* **66** 911
[16] Celestini F, Pellenq R J-M, Bordarier P and Rousseau B 1996 *Z. Phys.* D **37** 49
[17] Broughton J 1992 *Phys. Rev.* B **46** 2523
[18] Lutsko J F, Wolf D, Phillpot S R and Yip S 1989 *Phys. Rev.* B **40** 2841
[19] King H K 1970 *Physical Metallurgy* ed R W Cahn (Amsterdam: North-Holland) pp 59–63
[20] Mitch M G, Chase S J, Fortner J, Yu R Q and Lannin J S 1991 *Phys. Rev. Lett.* **67** 875
[21] Ajayan P M and Iijima S 1993 *Nature* **361** 233
[22] Mott N F 1934 *Proc. R. Soc.* A **146** 465
[23] Regel' R and Glazov V M 1995 *Semiconductors* **29** 405
[24] Jiang Q, Zhang Z and Li J C 2000 *Chem. Phys. Lett.* **286** 139
[25] Sambles J R 1971 *Proc. R. Soc.* A **324** 339
[26] Ben-David T, Lereah Y, Deutscher G, Kofman R and Cheyssac P 1995 *Phil. Mag.* A **71** 1135
[27] Skripov V P, Koverda V P and Skokov V N 1981 *Phys. Status Solidi* a **66** 109
[28] Eckert J, Holzer J C, Ahn C C, Fu Z and Johnson W L 1993 *Nanostr. Mater.* **2** 407
[29] Allen G L, Bayles R A, Gile W W and Jesser W A 1986 *Thin Solid Films* **144** 297
[30] Allen G L, Gile W W and Jesser W A 1980 *Acta. Metall.* **28** 1695
[31] Graback L and Bohr J 1990 *Phys. Rev. Lett.* **64** 934
[32] Saka H, Nishikawa Y and Imura T 1988 *Phil. Mag.* A **57** 895
[33] Lu K, Sheng H W and Jin Z H 1997 *Chinese J. Mater. Res.* **11** 658 (in Chinese)
[34] 1980 *Table of Periodic Properties of the Elements* (Skokie: Sargent-Welch Scientific Company) p 1